

Anandamide Hydrolysis by Human Cells in Culture and Brain*

(Received for publication, July 6, 1998, and in revised form, August 18, 1998)

Mauro Maccarrone‡§, Marcelis van der Stelt¶, Antonello Rossi‡§, Gerrit A. Veldink¶, Johannes F. G. Vliegthart¶, and Alessandro Finazzi Agrò‡§||

From the ‡Department of Experimental Medicine and Biochemical Sciences, University of Rome Tor Vergata, Via di Tor Vergata 135, I-00133 Rome, Italy, the §Istituto di Ricovero e Cura a Carattere Scientifico Centro S. Giovanni di Dio, Fatebenefratelli, I-25100 Brescia, Italy, and the ¶Bijvoet Center for Biomolecular Research, Department of Bio-organic Chemistry, Utrecht University, Padualaan 8, NL-3584 CH Utrecht, The Netherlands

Anandamide (arachidonylethanolamide; AnNH) has important neuromodulatory and immunomodulatory activities. This lipid is rapidly taken up and hydrolyzed to arachidonate and ethanolamine in many organisms. As yet, AnNH inactivation has not been studied in humans. Here, a human brain fatty-acid amide hydrolase (FAAH) has been characterized as a single protein of 67 kDa with a pI of 7.6, showing apparent K_m and V_{max} values for AnNH of $2.0 \pm 0.2 \mu M$ and $800 \pm 75 \text{ pmol} \cdot \text{min}^{-1} \cdot \text{mg}$ of protein $^{-1}$, respectively. The optimum pH and temperature for AnNH hydrolysis were 9.0 and 37 °C, respectively, and the activation energy of the reaction was $43.5 \pm 4.5 \text{ kJ} \cdot \text{mol}^{-1}$. Hydro(pero)xides derived from AnNH or its linoleoyl analogues by lipoxygenase action were competitive inhibitors of human brain FAAH, with apparent K_i values in the low micromolar range. One of these compounds, linoleoylethanolamide is the first natural inhibitor ($K_i = 9.0 \pm 0.9 \mu M$) of FAAH as yet discovered. An FAAH activity sharing several biochemical properties with the human brain enzyme was demonstrated in human neuroblastoma CHP100 and lymphoma U937 cells. Both cell lines have a high affinity transporter for AnNH, which had apparent K_m and V_{max} values for AnNH of $0.20 \pm 0.02 \mu M$ and $30 \pm 3 \text{ pmol} \cdot \text{min}^{-1} \cdot \text{mg}$ of protein $^{-1}$ (CHP100 cells) and $0.13 \pm 0.01 \mu M$ and $140 \pm 15 \text{ pmol} \cdot \text{min}^{-1} \cdot \text{mg}$ of protein $^{-1}$ (U937 cells), respectively. The AnNH carrier of both cell lines was activated up to 170% of the control by nitric oxide.

Anandamide (arachidonylethanolamide; AnNH)¹ is an endogenous lipid that binds to cannabinoid CB1 and CB2 receptors, which are mainly found in the central nervous system and in peripheral immune cells. It mimics the pharmacological effects of Δ^9 -tetrahydrocannabinol, the active principle of hashish and marijuana (1, 2). AnNH formation occurs mainly through phosphodiesterase-mediated cleavage of N-arachido-

noylphosphatidylethanolamine (3, 4), although a direct synthesis from arachidonic acid and ethanolamine has also been described (5, 6). AnNH can be released from depolarized neurons (3). Upon binding to CB1 receptors, AnNH induces inhibition of forskolin-induced cAMP accumulation, inhibition of N-type Ca^{2+} channels, and activation of mitogen-activated protein kinase signal transduction pathway (reviewed in Ref. 7) and increases protein tyrosine phosphorylation (8). Activation of the CB2 receptor leads to inhibition of adenylate cyclase and activation of the mitogen-activated protein kinase signaling (9). Interestingly, AnNH binding to cannabinoid receptors is coupled to nitric oxide (NO) release in the central nervous system of invertebrates and in peripheral immune cells of both invertebrates and humans (10).

The pharmacological effects of AnNH on CB1 and CB2 receptors depend on the life span of the lipid in the extracellular space, which is limited by a rapid and selective process of cellular uptake, followed by intracellular degradation of AnNH to ethanolamine and arachidonic acid by the enzyme fatty-acid amide hydrolase (FAAH). Both components of the inactivation process of AnNH are the subject of active investigation. AnNH uptake has been characterized in rat neuronal cells (3, 11, 12) and rat basophilic leukemia (RBL-2H3) cells (13). FAAH has been demonstrated and partially characterized in rat, porcine, and dog brains (14–16). Furthermore, FAAH activity has been shown in one “neuronal” cell line, namely mouse neuroblastoma N₁₈TG₂ (17), and in one “non-neuronal” cell line, namely RBL-2H3 (13). The FAAH gene has recently been cloned from rat, mouse, and human liver cDNAs, allowing molecular mass determination and substrate specificity analysis of the enzyme (18, 19). As yet, no information is available on the activity of human FAAH or on AnNH uptake in human cells. This prompted us to investigate some biochemical properties of FAAH from human brain and human neuronal and immune cells, *i.e.* neuroblastoma CHP100 and lymphoma U937 cells. AnNH uptake was characterized in these two cell types to gain information on the AnNH inactivation process in humans. The cell lines chosen are widely used as experimental models for neuronal (20) and immune (21) tissues. In these two cell types, AnNH uptake was demonstrated and characterized.

Taken together, the results reported here represent the first biochemical characterization of human brain FAAH. Most properties of this enzyme are shared by FAAH found in human neuronal and immune cells in culture. Remarkably, both cell lines seem to inactivate AnNH in the same way, which strengthens the concept of a neuroimmune axis in humans, which is evident, for instance, in the “axon-reflex” model for neurogenic inflammation (13). Possible implications of FAAH activity and expression in brain pathology are also discussed.

* This work was supported in part by the Istituto Superiore di Sanità (X AIDS Program) and the Ministero dell'Università e della Ricerca Scientifica e Tecnologica, Rome (to A. F. A.). The costs of publication of this article were defrayed in part by the payment of page charges. This article must therefore be hereby marked “advertisement” in accordance with 18 U.S.C. Section 1734 solely to indicate this fact.

|| To whom correspondence should be addressed. Tel. and Fax: 3906-72596468; E-mail: Finazzi@utovrm.it.

¹ The abbreviations used are: AnNH, anandamide (arachidonylethanolamide); NO, nitric oxide; FAAH, fatty-acid amide hydrolase; PMSF, phenylmethylsulfonyl fluoride; CCCP, carbonyl cyanide *m*-chlorophenylhydrazide; SNP, sodium nitroprusside; (13-H)ODNH₂OH, (13-hydroxy)-linoleoylethanolamide; (13H)-ODNH₂, (13-hydroxy)linoleoylamide; (13H)ODNHMe, (13-hydroxy)linoleoylmethylamide; 15/11-H(P)AnNH, 15/11-hydro(pero)xyanandamide; HPLC, high performance liquid chromatography; ELISA, enzyme-linked immunosorbent assay; RT-PCR, reverse transcriptase polymerase chain reaction.

EXPERIMENTAL PROCEDURES

Materials—Chemicals were of the purest analytical grade. Anandamide (arachidonyl ethanolamide), arachidonic acid, ethanolamine, phenylmethylsulfonyl fluoride (PMSF), iodoacetic acid, *N*-ethylmaleimide, carbonyl cyanide *m*-chlorophenylhydrazone (CCCP), and sodium nitroprusside (SNP) were purchased from Sigma. *S*-Nitroso-*N*-acetylpenicillamine was from Research Biochemicals International, and spermine NONOate ((*Z*)-1-[*N*-(3-aminopropyl)-*N*-[4-(3-aminopropylammonio)butyl]amino]diazene-1-ium-1,2-diolate) was from Alexis Corp. (Läufelfingen, Switzerland). Leukotriene B₄ and prostaglandin E₂ were from Cayman Chemical Co., Inc. [$1\text{-}^{14}\text{C}$]AnNH was synthesized from ethanolamine and [$1\text{-}^{14}\text{C}$]arachidonic acid (52 mCi/mmol; NEN DuPont de Nemours, Köln, Germany) as reported (22). Linoleylethanolamide ((9*Z*,12*Z*)-octadeca-9,12-dienylethanolamide; ODNHEtOH), linoleoylamide ((9*Z*,12*Z*)-octadeca-9,12-dienoylamide; ODNH₂), linoleoylmethylamide ((9*Z*,12*Z*)-octadeca-9,12-dienoylmethylamide; ODNHMe), and their 13-hydroxy derivatives (13-HODNHEtOH, 13-HODNH₂, and 13-HODNHMe) were synthesized and characterized (purity >96% by gas-liquid chromatography) as reported (23). 15-Hydro(pero)xyanandamide (15-hydro(pero)xyeicosa-(5*Z*,8*Z*,11*Z*,13*E*)-tetraenylethanolamide; 15-H(P)AnNH; purity >96%) and 11-hydro(pero)xyanandamide (11-H(P)AnNH; a mixture of 45% 11-H(P)AnNH, 24% 5-H(P)AnNH, 18% 15-H(P)AnNH, 9% 8/9-H(P)AnNH, and 4% 12-H(P)AnNH by reversed-phase high performance liquid chromatography) were a gift from Guus van Zadelhof (Bijvoet Center for Biomolecular Research, Utrecht University).

Biological Material—Human brain specimens were obtained from five different male patients (aged 73–77) undergoing surgical operations to remove meningioma tumors. Brain tissues were removed and donated by Prof. R. Giuffrè and Dr. G. De Caro (Neurosurgery Division, University of Rome Tor Vergata, Sant'Eugenio Hospital, Rome, Italy). In four cases, the perilesional white matter surrounding the tumor area was removed (1 g of fresh tissue in total) and used for FAAH characterization. In one case, both meningioma and perilesional white matter (0.1 g of each fresh tissue) were removed and used to compare FAAH activity and expression in meningioma and healthy brain.

Human neuroblastoma CHP100 cells were cultured as reported (20) in a 1:1 mixture of Eagle's minimal essential medium plus Earle's salts and Ham's F-12 medium (Flow Laboratories Ltd., Irvine, United Kingdom) supplemented with 15% heat-inactivated fetal bovine serum, 1.2 g/liter sodium bicarbonate, 15 mM Hepes, 2 mM L-glutamine, and 1% nonessential amino acids. Human lymphoma U937 cells, a gift from Dr. E. Faggioli (Department of Public Health and Cell Biology, University of Rome Tor Vergata), were cultured in RPMI 1640 medium (Gibco, Paisley, United Kingdom) supplemented with 25 mM Hepes, 2.5 mM sodium pyruvate, 100 units/ml penicillin, 100 µg/ml streptomycin, and 10% heat-inactivated fetal calf serum (21). Both CHP100 and U937 cells were maintained at 37 °C in a humidified 5% CO₂ atmosphere.

Assay of FAAH—Immediately after surgical removal, human brain specimens were washed in phosphate-buffered saline and homogenized with an UltraTurrax T25 in 50 mM Tris-HCl and 1 mM EDTA, pH 7.4 (buffer A), at a 1:10 homogenization ratio (fresh weight/volume). Membranes from these tissue homogenates were then prepared as described (15, 17). The final pellet, containing most of the FAAH activity (13, 17, 24), was resuspended in ice-cold buffer A at a protein concentration of 1 mg/ml and stored at –80 °C until use. Both CHP100 and U937 cells (3 × 10⁸/sample) were collected in phosphate-buffered saline and centrifuged at 1000 × *g* for 10 min. The dry pellet was resuspended in 30 ml of ice-cold buffer A and sonicated on ice three times for 10 s, with 10-s intervals, using a Vibracell sonifier (Sonics & Materials Inc.) with a microtip at maximum power. The homogenate was then centrifuged sequentially as described above for the human brain, and the final pellet was stored at –80 °C in buffer A at a protein concentration of 1 mg/ml until use.

The assay of FAAH (arachidonyl ethanolamide amidohydrolase, EC 3.5.1.4) activity was performed by reversed-phase high performance liquid chromatography (HPLC) as recently described (22). Thermal stability and pH dependence of FAAH activity were studied as described (17). Activation energy values were calculated as reported (25). Kinetic and inhibition studies were performed using different concentrations of [$1\text{-}^{14}\text{C}$]AnNH (in the 0–21 µM range) and two different concentrations (10 and 20 µM) of each inhibitor to calculate the kinetic parameters. Fitting of the experimental points to a Lineweaver-Burk plot by a linear regression program (Kaleidagraph Version 3.0) yielded straight lines with *r* values >0.95.

The assay of the FAAH synthase activity was performed by measuring the formation of [$1\text{-}^{14}\text{C}$]AnNH from [$1\text{-}^{14}\text{C}$]arachidonic acid and ethanolamine as reported (5). Tissue or cell homogenates (20 µg of proteins/test) were incubated for 15 min at 37 °C in 200 µl of 50 mM

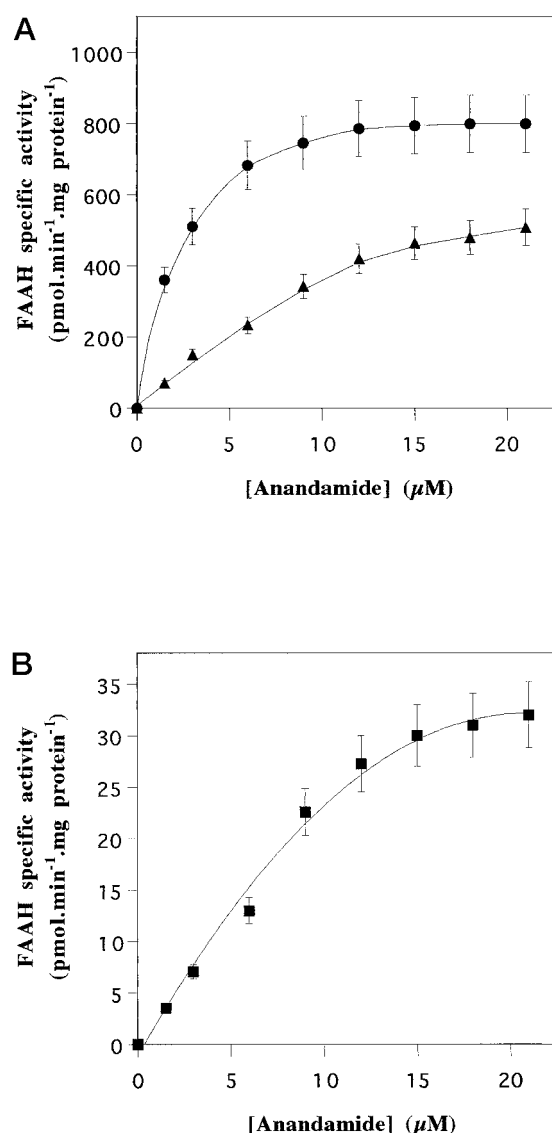


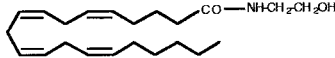
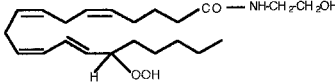
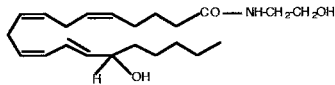
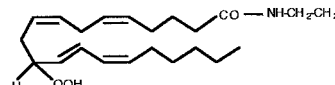
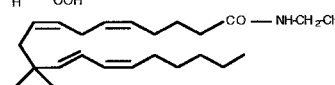

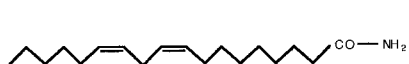

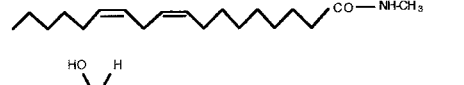
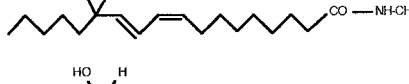
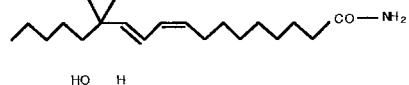
FIG. 1. Dependence of FAAH activity on anandamide concentration. In A, FAAH activity was assayed at various anandamide concentrations in human brain (●) and human lymphoma U937 cells (▲) in culture. In B, FAAH activity was assayed in human neuroblastoma CHP100 cells (■) in culture. In both panels, FAAH activity was measured at pH 9.0 and 37 °C.

Tris-HCl, pH 9.0, containing 10 µM [$1\text{-}^{14}\text{C}$]arachidonic acid (52 mCi/mmol) and 2 mM ethanolamine. The reaction was stopped, and the products were extracted and analyzed by reversed-phase HPLC following the same procedure as described above for the hydrolase activity. FAAH synthase activity is expressed as picomoles of AnNH formed per min/mg of protein. The effect of various compounds on the hydrolase or synthase activity of FAAH was determined by adding each substance directly to the assay buffer at the indicated concentrations.

Immunochemical Analysis—SDS-polyacrylamide gel electrophoresis (12%) was performed under reducing conditions in a Mini-Protein II apparatus (Bio-Rad) with 0.75-mm spacer arms (26). Rainbow molecular mass markers (Amersham International, Buckinghamshire, United Kingdom) were phosphorylase *b* (97.4 kDa), bovine serum albumin (66.0 kDa), and ovalbumin (46.0 kDa). Native isoelectric focusing was performed in the Mini-Protein II apparatus using a 5% polyacrylamide gel containing ampholytes in the pH range 5.0–9.0 (Sigma) as described (27). Isoelectric focusing was calibrated by running the following pI markers (Sigma): lentil (*Lens culinaris*) lectin (pI 8.8, 8.6, and 8.2), myoglobin from horse heart (pI 7.2 and 6.8), carbonic anhydrase I from human erythrocytes (pI 6.6), and carbonic anhydrase II from bovine erythrocytes (pI 5.9). Human brain homogenates (20 µg/lane), prepared as described above for FAAH assay, were subjected to either SDS-

TABLE I
Inhibition of human brain FAAH activity by different anandamide products and analogues

Apparent inhibition constant (K_i) values were calculated by Lineweaver-Burk profiles of AnNH hydrolysis by FAAH. All compounds were reversible competitive inhibitors of FAAH activity. Total activity of human brain FAAH was determined using 10 μ M AnNH or congeners as substrate.

Structure of the compound	Inhibition constant (K_i , μ M)	Total activity (%)
 (AnNH)	None	100 ^a
 (15-HPAnNH)	4.8 \pm 0.5	80 \pm 8
 (15-HAnNH)	3.2 \pm 0.3	82 \pm 8
 (11-HPAnNH) ^b	5.2 \pm 0.5	83 \pm 8
 (11-HAnNH) ^c	4.0 \pm 0.4	85 \pm 9
 (ODNHEtOH)	9.0 \pm 0.9	76 \pm 8
 (ODNH ₂)	14.1 \pm 1.3	70 \pm 7
 (ODNHMe)	24.5 \pm 2.1	72 \pm 7
 (13-HODNHEtOH)	3.0 \pm 0.3	56 \pm 6
 (13-HODNH ₂)	5.3 \pm 0.5	49 \pm 5
 (13-HODNHMe)	9.3 \pm 0.9	50 \pm 5

^a 100% = 750 \pm 70 pmol \cdot min⁻¹ \cdot mg of protein⁻¹.

^b 11-HPAnNH was a mixture of 11-HPAnNH (45%), 5-HPAnNH (24%), 15-HPAnNH (18%), 8/9-HPAnNH (9%), and 12-HPAnNH (4%).

^c 11-HAnNH was the same mixture as 11-HPAnNH, reduced with NaBH₄.

polyacrylamide gel electrophoresis or isoelectric focusing, and then slab gels were electroblotted onto 0.45- μ m nitrocellulose filters (Bio-Rad) using a Mini-TransBlot apparatus (Bio-Rad) as reported (26). Immunodetection of FAAH on nitrocellulose filters was performed with specific anti-FAAH polyclonal antibodies (diluted 1:200), raised in rabbits against the conserved FAAH sequence VGYETDNYTMPSPAMR (19), conjugated to ovalbumin. This peptide antigen and the anti-FAAH polyclonal antibodies were prepared by Primm s. r. l. (Milan, Italy). Goat anti-rabbit alkaline phosphatase conjugate (Bio-Rad; diluted 1:2000) was used as secondary antibody, and immunoreactive bands were stained with the alkaline phosphatase staining solution according to the manufacturer's instructions (Bio-Rad).

Enzyme-linked immunosorbent assay (ELISA) was performed by coating the plate with human brain homogenate (20 μ g/well), prepared as described above for the FAAH assay. Anti-FAAH polyclonal antibodies were used as primary antibody (diluted 1:300), and goat anti-rabbit alkaline phosphatase conjugate as secondary antibody (diluted 1:2000). Color development of the alkaline phosphatase reaction was measured at 405 nm using *p*-nitrophenyl phosphate as substrate. For peptide competition experiments, the peptide antigen was preincubated with a 1000-fold molar excess of anti-FAAH polyclonal antibodies for 30 min at room temperature before adding the antibodies to the wells (18). Con-

trols were carried out using non-immune rabbit serum and included wells coated with different amounts of bovine serum albumin.

Reverse Transcriptase Polymerase Chain Reaction (RT-PCR) and Sequencing—2–5 \times 10⁶ cells or 20 mg of tissue were used to isolate total RNA by means of the S.N.A.P.TM total RNA isolation kit (Invitrogen). Control reactions were carried out to ensure complete removal of genomic DNA. RT-PCRs were performed using the EZ rTth RNA PCR kit (Perkin-Elmer) following the manufacturer's instructions. The reaction conditions were carefully examined to stop the reaction during the exponential phase of amplification of each gene. Briefly, 100 ng (for the amplification of FAAH) or 0.4 ng (for 18 S rRNA) of total RNA were reversibly transcribed and amplified in the same tube in a total reaction volume of 10 μ l in the presence of 3 mCi of [α -³²P]dCTP (3000 Ci/mmol; Amersham International). The amplification parameters were as follows: 2 min at 95 $^{\circ}$ C, 45 s at 95 $^{\circ}$ C, 30 s at 55 $^{\circ}$ C, and 30 s at 60 $^{\circ}$ C. Linear amplification was observed after 20 cycles. The primers were as follows: (+)5'-TGGAAGTCCTCCAAAAGCCCAG and (–)5'-TGTC-CATAGACACAGCCCTTCAG for FAAH and (+)5'-AGTTGCTGCAGT-TAAAAAGC and (–)5'-CCTCAGTTCCGAAAACCAAC for 18 S rRNA.

Five μ l of the reaction mixture were electrophoresed on a 6% polyacrylamide gel, which was then dried and subjected to autoradiography. Products were validated by size determination and sequencing. For

quantitation of the RT-PCR products, bands were excised from the gel and counted in an LKB1214 Rackbeta scintillation counter (Amersham Pharmacia Biotech, Uppsala, Sweden). Linear amplification sequencing was performed using a Cyclist™ DNA sequencing kit (Stratagene) according to the manufacturer's instructions. RT-PCR products for sequencing were prepared without [α - 32 P]dCTP and sequenced with the same primers used for amplification after labeling them with [γ - 32 P]dATP (3000 Ci/mmol; Amersham International).

Determination of Anandamide Uptake—The uptake of [14 C]AnNH (52 mCi/mmol) in intact CHP100 or U937 cells was studied essentially as described (13). CHP100 and U937 cells were resuspended in their serum-free culture media at a density of 1×10^6 cells/ml. Cell suspensions (2 ml/test) were incubated for different time intervals at 37 °C with 100 nM [14 C]AnNH; then they were washed three times in 2 ml of culture medium containing 1% bovine serum albumin and were finally resuspended in 200 μ l of phosphate-buffered saline. Membrane lipids were then extracted (28), resuspended in 0.5 ml of methanol, and mixed with 3.5 ml of Sigma-Fluor liquid scintillation mixture for non-aqueous samples (Sigma), and radioactivity was measured in an LKB1214 Rackbeta scintillation counter. To discern non-protein-mediated from protein-mediated transport of AnNH into cell membranes, control experiments were carried out at 4 °C (13). Incubations (15 min) were also carried out with different concentrations of [14 C]AnNH (in the 0–750 nM range) to determine apparent K_m and V_{max} of the uptake by Lineweaver-Burk analysis (in this case, the uptake at 4 °C was

subtracted from that at 37 °C). The Q_{10} value was calculated as the ratio of AnNH uptake at 30 and 20 °C (11). AnNH uptake is expressed as picomoles of AnNH taken up per min/mg of protein. The effect of different compounds on AnNH uptake was determined by adding each substance directly to the incubation medium at the indicated concentrations. In the case of CCCP, cells were preincubated with 50 μ M CCCP for 15 min at 37 °C before the addition of [14 C]AnNH to abolish mitochondrial transmembrane potential (29). Cell viability after each treatment was checked with trypan blue and found to be higher than 90% in all cases. It is noteworthy that no specific binding of [3 H]CP55940, a potent cannabinoid, was obtained with plasma membranes of CHP100 cells,² and U937 cells express hardly detectable levels of CB1 mRNA and very low levels of CB2 mRNA (21); thus, [14 C]AnNH binding to CB receptors is not likely to interfere in the uptake experiments (11, 13).

Data Analysis—Data reported in this paper are the means \pm S.D. of at least three independent determinations, each performed in duplicate. Statistical analysis was performed by the Student's *t* test, elaborating experimental data by means of the InStat program (GraphPAD Software for Science).

RESULTS

Characterization of FAAH in Human Brain and Human CHP100 and U937 Cells—Pilot experiments indicated that human brain FAAH activity was linearly dependent on the amount of tissue homogenate (in the range 0–30 μ g of protein) and the incubation time of the reaction (in the range 0–30 min), whereas it depended on AnNH concentration according to Michaelis-Menten kinetics (Fig. 1A) (data not shown), yielding an apparent K_m of 2.0 ± 0.2 μ M and a V_{max} of 800 ± 75 pmol·min⁻¹·mg of protein⁻¹. The activity of FAAH was assayed in the pH range 5.0–11.0 and in the temperature range 20–65 °C, showing an optimum pH and temperature at 9.0 and 37 °C, respectively. Arrhenius diagrams of AnNH hydrolysis by FAAH in the temperature range 20–45 °C allowed us to calculate an activation energy of 43.5 ± 4.5 kJ·mol⁻¹.

Hydroxylated AnNH derivatives and the linoleoyl analogues of AnNH were competitive inhibitors of human brain FAAH, with apparent K_i values ranging from 3.2 to 24.5 μ M (Table I).

² M. Maccarrone, A. M. Paoletti, G. Bagetta, and A. Finazzi Agrò, unpublished results.

Human brain FAAH

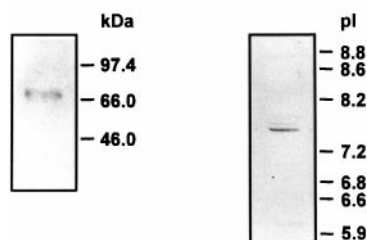


FIG. 2. **Electrophoretic properties of human brain FAAH.** Human brain extracts (20 μ g/lane) were subjected to either SDS-polyacrylamide gel electrophoresis (left panel) or isoelectric focusing (right panel). Slab gels were then electroblotted onto nitrocellulose filters, and FAAH was detected as an immunoreactive band with specific anti-FAAH polyclonal antibodies. Molecular mass markers and pI markers are shown.

TABLE II

Inhibition of FAAH activity and [14 C]anandamide uptake in human brain and human CHP100 and U937 cells

FAAH activity was determined using 10 μ M AnNH as substrate. For uptake experiments, cells (2×10^6) were incubated for 15 min at 37 °C with 100 nM [14 C]AnNH in the presence of each compound. Activity and uptake values are expressed as percentage of the untreated controls, arbitrarily set to 100 (see below for absolute values). Results on FAAH activity in CHP100 and U937 cells were superimposable; thus, FAAH activity in CHP100 cells was omitted for the sake of clarity.

Compound	FAAH activity		Anandamide uptake	
	Brain	U937	CHP100	U937
	%		%	
None	100 ^a	100 ^b	100 ^c	100 ^d
Arachidonic acid (100 μ M)	18 \pm 2	16 \pm 2	100 \pm 10	100 \pm 10
Ethanolamine (100 μ M)	83 \pm 8	80 \pm 8	95 \pm 10	88 \pm 9
15-HAnNH (10 μ M)	33 \pm 3	50 \pm 5	90 \pm 9	87 \pm 9
ODNHEtOH (10 μ M)	56 \pm 6	62 \pm 6	89 \pm 9	85 \pm 9
13-HODNHEtOH (10 μ M)	26 \pm 3	43 \pm 4	80 \pm 8	82 \pm 8
Leukotriene B ₄ (1 μ M)	ND ^e	ND	105 \pm 10	100 \pm 10
Prostaglandin E ₂ (10 μ M)	ND	ND	105 \pm 10	105 \pm 10
PMSF (100 μ M)	6 \pm 1	8 \pm 1	50 \pm 5	52 \pm 5
Iodoacetic acid (100 μ M)	10 \pm 1	12 \pm 1	50 \pm 5	48 \pm 5
N-Ethylmaleimide (100 μ M)	15 \pm 2	18 \pm 2	55 \pm 5	50 \pm 5
CCCP (50 μ M)	ND	ND	85 \pm 9	86 \pm 9
SNP (5 mM)	87 \pm 9	85 \pm 9	170 \pm 17	See Fig. 5B
SNAP (5 mM)	85 \pm 9	87 \pm 9	175 \pm 18	See Fig. 5B
SPER-NO (5 mM)	88 \pm 9	84 \pm 9	172 \pm 17	See Fig. 5B

^a 100% = 750 ± 70 pmol·min⁻¹·mg of protein⁻¹.

^b 100% = 390 ± 40 pmol·min⁻¹·mg of protein⁻¹.

^c 100% = 7.0 ± 0.7 pmol·min⁻¹·mg of protein⁻¹.

^d 100% = 53.0 ± 5.5 pmol·min⁻¹·mg of protein⁻¹.

^e ND, not determined; SNAP, S-nitroso-N-acetylpenicillamine; SPER-NO, spermine NONOate.

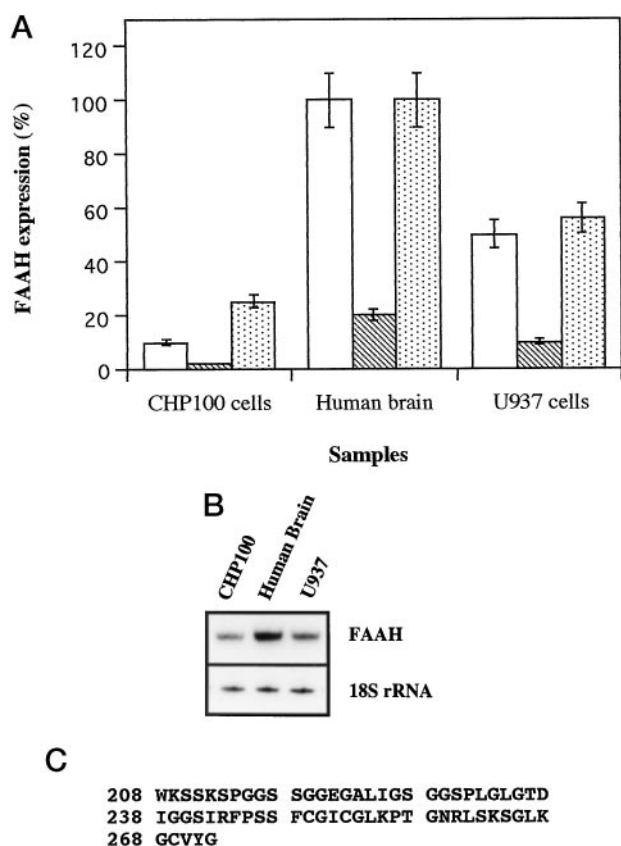


FIG. 3. Quantitation of FAAH in human brain and human CHP100 and U937 cells. *A*, tissue or cell homogenates (20 μ g/well) were subjected to ELISA using specific anti-FAAH polyclonal antibodies (white bars). Antigen competition ELISA (hatched bars) was performed by preincubating anti-FAAH polyclonal antibodies with a 1000-fold molar excess of peptide antigen. Absorbance values are expressed as percentage of the maximum, arbitrarily set to 100 (100% corresponds to 0.760 ± 0.080 absorbance units at 405 nm). FAAH mRNA levels (dotted bars) were quantitated by liquid scintillation counting and are expressed as percentage of the maximum, arbitrarily set to 100 (100% = $20,000 \pm 2000$ cpm). The radioactivity of the bands corresponding to 18 S rRNA (see *B*) was identical in all samples (5000 ± 500 cpm). *B*, FAAH mRNA (50 ng/lane) and 18 S rRNA (0.2 ng/lane) were amplified by RT-PCR and electrophoresed on 6% polyacrylamide gels. *C*, shown is the conserved amino acid sequence deduced from FAAH mRNA isolated from human brain or human CHP100 or U937 cells. The sequence contains the amidase consensus sequence (amino acids 215–246) typical of all FAAHs as yet known.

These AnNH congeners were also alternate substrates of FAAH, yielding total activities that ranged from 85% (11-HAnNH) to 49% (13-HODNH₂) of the activity obtained with AnNH itself (Table I). The substrate specificity of FAAH from human brain resembled that of the enzyme from mouse or rat brain (18, 19, 22).

Western blotting showed that anti-FAAH polyclonal antibodies specifically recognized a single immunoreactive band in brain homogenates, corresponding to a molecular mass of ~67 kDa and an isoelectric point of ~7.6 (Fig. 2).

Human neuronal (CHP100) and immune (U937) cells in culture also showed FAAH activity, with pH and temperature profiles superimposable to those observed with the human brain enzyme (data not shown). Both cell lines showed an FAAH activity (Fig. 1, *A* and *B*) characterized by apparent K_m and V_{max} values of 6.5 ± 0.6 μ M and 32 ± 3 pmol·min⁻¹·mg of protein⁻¹ (CHP100) and 6.5 ± 0.6 μ M and 520 ± 50 pmol·min⁻¹·mg of protein⁻¹ (U937) for AnNH. The activation energy of AnNH hydrolysis by FAAH in CHP100 or U937 cells

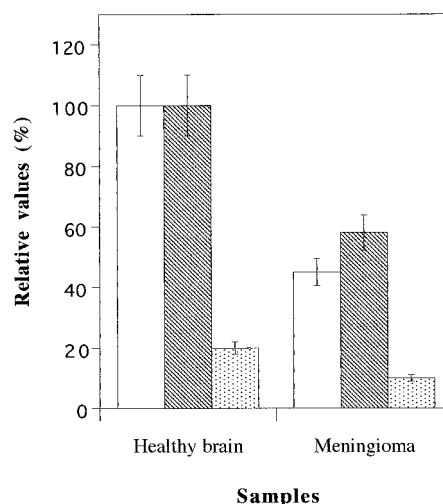


FIG. 4. Comparison of FAAH activity and expression in human healthy brain and meningioma. FAAH activity (white bars) was measured using 10 μ M AnNH as substrate. FAAH protein content (hatched bars) was determined by ELISA using 20 μ g of proteins/well. Antigen competition ELISA (dotted bars) was performed by preincubating anti-FAAH polyclonal antibodies with a 1000-fold molar excess of peptide antigen. FAAH activity and content are expressed as percentage of the control (healthy brain), arbitrarily set to 100 (100% = 750 ± 70 pmol·min⁻¹·mg of protein⁻¹ for the activity; 100% = 0.760 ± 0.080 absorbance units at 405 nm for the protein content).

(45.0 ± 4.5 kJ·mol⁻¹ in either case) was the same as the human brain enzyme. Moreover, 15-HAnNH, ODNHEtOH, and 13-HODNHEtOH competitively inhibited FAAH activity in both cell lines, with apparent K_i values of 4.5 ± 0.4 , 11.1 ± 0.9 , and 6.1 ± 0.5 μ M (CHP100) and 3.8 ± 0.4 , 10.5 ± 1.0 , and 4.5 ± 0.4 μ M (U937), respectively. Excess (100 μ M) arachidonic acid, but not ethanolamine, strongly inhibited FAAH activity in all human sources tested, in line with previous findings on mouse FAAH (17). Alkylating agents such as PMSF, iodoacetic acid, and *N*-ethylmaleimide (at 100 μ M) almost abolished FAAH activity in all sources (Table II). The NO donors SNP, *S*-nitroso-*N*-acetylpenicillamine, and spermine NONOate (at millimolar concentrations that release nanomolar concentrations of NO in solution) (30, 31) hardly affected the hydrolase activity (Table II).

An anandamide synthase activity (32) was also present in the materials from human sources. The following maximum reaction rates were found: 70 ± 7 (human brain), 24.5 ± 2.5 (CHP100), and 40 ± 4 (U937) pmol·min⁻¹·mg of protein⁻¹. These values were ~5-fold (CHP100 cells) to 10-fold (human brain and U937 cells) lower than the hydrolase activity under the same assay conditions (*i.e.* 10 μ M arachidonic acid and 20 μ g of proteins), as shown in Fig. 1. Nevertheless, the synthase was affected by 15-HAnNH, ODNHEtOH, 13-HODNHEtOH, PMSF, and SNP in the same way as the hydrolase activity (Table II), both in human brain and human cell lines (data not shown).

Expression of FAAH in Human Brain and Human CHP100 and U937 Cells—The analysis of FAAH expression in human brain and human cells was performed at the protein (by ELISA) and mRNA (by RT-PCR) levels. The amount of FAAH protein in human brain was ~2- or 10-fold higher than that observed in U937 or CHP100 cells, respectively (Fig. 3A). This quantitation was validated by antigen competition experiments (18), showing that immunoreaction of the anti-FAAH polyclonal antibodies with the enzyme protein in human homogenates was specific (Fig. 3A). RT-PCR analysis showed similar differences in the mRNA levels (Fig. 3, *A* and *B*). Sequencing of

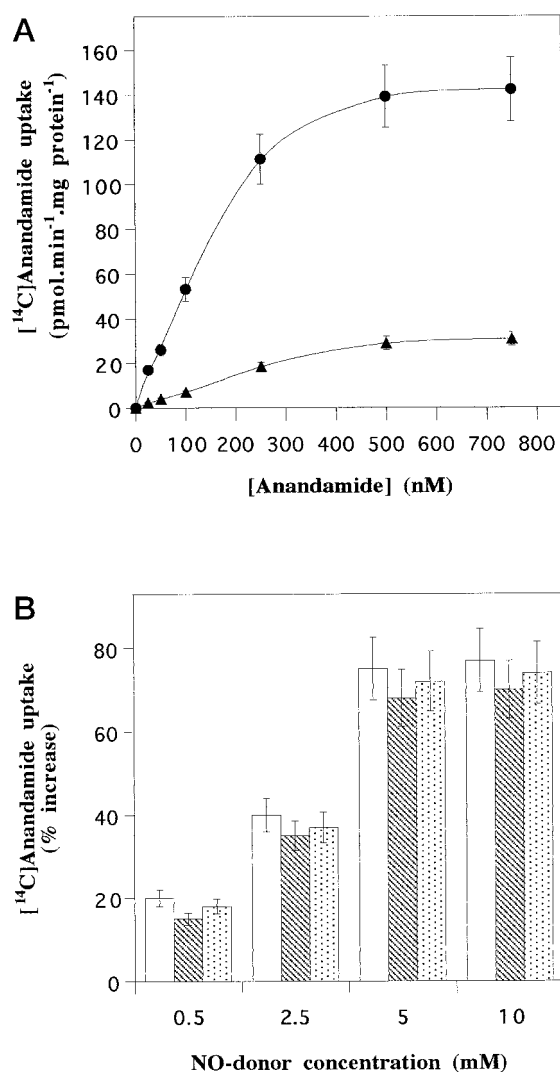


FIG. 5. Uptake of $[^{14}\text{C}]\text{anandamide}$ in intact CHP100 and U937 cells. A, dependence of $[^{14}\text{C}]\text{AnNH}$ uptake (15 min, 37°C) on AnNH concentration in human U937 (●) and CHP100 (▲) cells. B, effect of NO donors SNP (white bars), *S*-nitroso-*N*-acetylpenicillamine (hatched bars), and spermine NONOate (dotted bars) on the uptake of 100 nM $[^{14}\text{C}]\text{AnNH}$ in U937 cells (15 min, 37°C). Uptake increase is expressed as percentage over the untreated control (100% = $53.0 \pm 5.5 \text{ pmol}\cdot\text{min}^{-1}\cdot\text{mg of protein}^{-1}$).

TABLE III

Kinetic parameters of anandamide uptake in human CHP100 and U937 cells

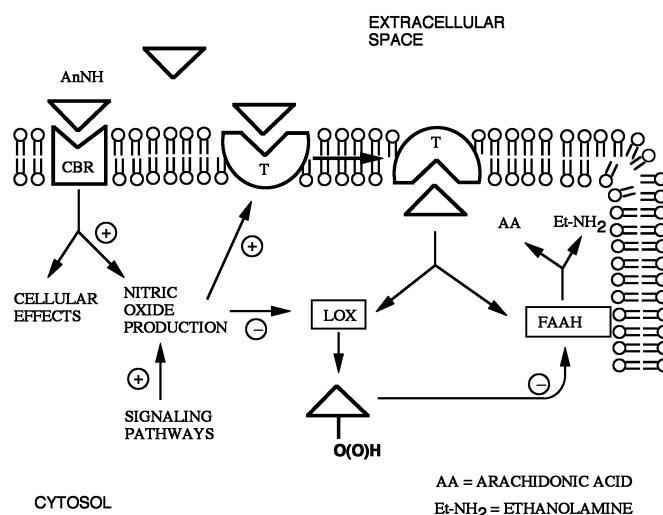
Uptake of $[^{14}\text{C}]\text{AnNH}$ was investigated in cell suspensions (2×10^6 cells/test), either untreated or treated with the NO donor SNP or the alkylating agent PMSF. Apparent K_m and V_{\max} values are expressed as micromolar and picomoles $\cdot \text{min}^{-1} \cdot \text{mg of protein}^{-1}$, respectively.

Human cell line	K_m	V_{\max}	V_{\max}/K_m
Neuroblastoma CHP100 cells	0.20 ± 0.02	30 ± 3	150
+5 mM SNP	0.20 ± 0.02	650 ± 5^a	250
+100 μM PMSF	0.20 ± 0.02	15 ± 2^a	75
Lymphoma U937 cells	0.13 ± 0.01	140 ± 15	1077
+5 mM SNP	0.13 ± 0.01	230 ± 22^a	1769
+100 μM PMSF	0.13 ± 0.01	75 ± 8^a	577

^a $p < 0.01$ compared with the control.

the FAAH mRNA, amplified by RT-PCR from human brain or human CHP100 or U937 cells, showed that human FAAH possesses a completely conserved sequence between amino acids 208 and 272, which contains a typical amidase consensus sequence (Fig. 3C).

FAAH activity and expression were measured also in human



SCHEME 1. Interaction between anandamide uptake and degradation. Binding of extracellular AnNH to cannabinoid receptors (CBR) leads to intracellular NO production, which in turn activates transporter (T)-mediated uptake of AnNH. Once taken up, AnNH can be rapidly cleaved by membrane-bound FAAH, releasing arachidonic acid and ethanolamine. Alternatively, hydro(pero)xides of AnNH can be generated by lipoxygenase (LOX) activity, leading to inhibition of FAAH. This alternate pathway is prevented by NO, short pulses of which are able to inhibit lipoxygenase activity. It should be stressed that other signaling pathways, uncoupled to AnNH binding to CBR receptors, can enhance intracellular production of NO, thus activating the sequestration process of this lipid mediator. Therefore, cannabinoid-binding receptors can reside on the same cell bearing the inactivation machinery or on different cells.

meningioma and were compared with those found in the perilesional white matter (healthy brain). AnNH hydrolysis by meningioma FAAH followed Michaelis-Menten kinetics, with apparent K_m and V_{\max} values of $4.0 \pm 0.4 \mu\text{M}$ and $370 \pm 40 \text{ pmol}\cdot\text{min}^{-1}\cdot\text{mg of protein}^{-1}$, respectively. Interestingly, the specific activity of FAAH in human meningioma was 50% compared with that in healthy brain, a value that was paralleled by the amount of FAAH protein in the same tissues (Fig. 4).

Characterization of AnNH Uptake in Human CHP100 and U937 Cells—Neuroblastoma CHP100 and lymphoma U937 cells were able to accumulate $[^{14}\text{C}]\text{AnNH}$, a process that was temperature-dependent ($Q_{10} = 1.5$ for both cell lines), time-dependent ($t_{1/2} = 5 \text{ min}$ for both cell lines), and concentration-dependent (Fig. 5A) (data not shown). $[^{14}\text{C}]\text{AnNH}$ uptake in CHP100 and U937 cells was saturable ($K_m = 0.20 \pm 0.02$ and $0.13 \pm 0.01 \mu\text{M}$ and $V_{\max} = 30 \pm 3$ and $140 \pm 15 \text{ pmol}\cdot\text{min}^{-1}\cdot\text{mg of protein}^{-1}$, respectively); was enhanced when incubations were carried out in the presence of the NO donors SNP, *S*-nitroso-*N*-acetylpenicillamine, and spermine NONOate (Table II and Fig. 5B); and was reduced in the presence of PMSF, iodoacetic acid, or *N*-ethylmaleimide, each used at a 100 μM final concentration (Table II). Enhancement of $[^{14}\text{C}]\text{AnNH}$ uptake by 5 mM SNP was prevented by co-incubation with either 20 μM hemoglobin, a typical NO scavenger (20), or 100 μM PMSF (data not shown). SNP and PMSF affected the uptake kinetics by changing the V_{\max} value, but not the K_m , thus changing the catalytic efficiency (*i.e.* the V_{\max}/K_m ratio) of the transporter (Table III). On the other hand, 100 μM arachidonic acid or ethanolamine and 10 μM 15-HAnNH, ODNH₂OH, or 13-HODNH₂OH did not significantly influence AnNH uptake in either cell type, nor did 1 μM leukotriene B₄, 10 μM prostaglandin E₂, or 50 μM CCCP (Table II).

DISCUSSION

Meningioma is a histologically benign tumor that is brain-invasive only in 4% of cases (33). Thus, perilesional white

matter surrounding the meningioma can be considered an essentially healthy brain area and was chosen in this study to characterize FAAH. Human brain showed a remarkable FAAH activity, and anti-FAAH antibodies recognized a single protein of 67 kDa with an isoelectric point of 7.6, characterized here for the first time (Fig. 2). These values were in good agreement with the size of the full-length human liver FAAH cDNA (19) and the isoelectric point predicted from FAAH sequence by the GCG Sequence Analysis Software Package (46). Moreover, human brain FAAH cDNA had the same amidase consensus sequence (Fig. 3C) as FAAH cloned from human, mouse, and rat livers (18, 19). It is noteworthy that the activation energy of the AnNH hydrolysis catalyzed by FAAH from all three sources was identical. Furthermore, the FAAH activity in human CHP100 and U937 cells shared several other biochemical properties, such as pH and temperature dependence and inhibition profile, with the enzyme from human brain. In addition, the enzymes contained an identical amidase sequence. This might indicate that the same enzyme was present in all human samples, although the participation of other enzymes cannot be ruled out.

Human brain FAAH was further characterized with respect to its interaction with inhibitors. Here, linoleoyl analogues of AnNH and hydro(pero)xides generated thereof, which are likely to be produced *in vivo* by brain lipoxygenases (16, 22, 23, 34), were shown to be competitive inhibitors of FAAH activity, with apparent K_i values in the low micromolar range (Table I). Interestingly, linoleylethanolamide is a physiological constituent of rat neurons (3) and has recently been reported to displace [^3H]CP55940, a potent cannabinoid, only at high concentrations ($K_i > 1 \mu\text{M}$) from cannabinoid receptors in rat brain membranes (22). This compound might be the first natural inhibitor of FAAH as yet discovered. It has recently been shown, however, that oleamide, a sleep-inducing lipid, inhibited FAAH activity, but as high as 100 μM oleamide was needed to inhibit it by 50% in mouse neuroblastoma N₁₈TG₂ cells (24).

It is noteworthy that the apparent V_{max} of human brain FAAH was ~2- or 25-fold higher than that of U937 or CHP100 cells, respectively. The presence of different amounts of FAAH in the cells could explain this observation. Indeed, the amount of FAAH protein was 2- or 10-fold higher in human brain than in U937 or CHP100 cells, respectively (Fig. 3A), and similar differences were observed in the level of FAAH mRNA (Fig. 3B). Therefore, it can be suggested that a different expression (both at the transcriptional and translational level) of the same enzyme might be responsible for the different apparent V_{max} values of FAAH from the different human sources. A differential expression of FAAH might also be involved in human brain pathology, as suggested by comparison of meningioma and the surrounding (healthy) white matter (Fig. 4). This seems of interest if one recalls that a neurotrophic effect of AnNH has been proposed (8) and that AnNH might act as growth factor for hematopoietic cell lines (35, 36). Therefore, a lower expression of the AnNH-hydrolyzing enzyme FAAH might be instrumental in prolonging AnNH-associated growth stimulus, ultimately leading to cell immortalization.

To be inactivated by FAAH, AnNH has to be transported into the cell. Recent experiments performed on rat neuronal cells (3, 11, 12), rat basophilic leukemia (RBL-2H3) cells, and mouse J774 macrophages (13) clearly showed the presence of a high affinity AnNH transporter in the outer cell membranes. A similar methodology was used here to characterize, for the first time, the AnNH uptake in human neuronal (CHP100) and immune (U937) cells. Both cell types rapidly took up AnNH ($t_{1/2} = 5 \text{ min}$) in a temperature-dependent ($Q_{10} = 1.5$) and saturable way (Fig. 5A and data not shown). [^{14}C]AnNH was taken up by

CHP100 and U937 cells with similar high affinity, but remarkably different velocity (Table III). Interestingly, U937 cells, which possessed higher FAAH activity than CHP100 cells, showed also a more efficient AnNH uptake. The affinity of the AnNH transporter in human cells was comparable to that in rat astrocytes ($K_m = 0.32 \mu\text{M}$) (12) and was almost an order of magnitude higher than the affinity reported for dopamine ($K_m = 1 \mu\text{M}$) or glutamate ($K_m = 1\text{--}5 \mu\text{M}$) carriers in rat brain (37, 38). Furthermore, the uptake of AnNH in human cells was affected by AnNH hydrolysis products, leukotriene B₄, prostaglandin E₂, and alkylating agents (Table II) in much the same way as reported for rat neuronal and non-neuronal cells (11–13). This suggests that AnNH accumulation is selective and mediated by a transporter other than the long chain fatty acid transporter protein (39) or the prostaglandin transporter (40), in keeping with recent data on the AnNH carrier of rat neurons and astrocytes (12). AnNH uptake in human CHP100 and U937 cells was independent of mitochondrial energy metabolism because the uncoupling agent CCCP (29) hardly affected AnNH accumulation (Table II). These results indicate that AnNH is accumulated by a carrier-mediated facilitated diffusion, as recently reported for rat cells (11). The enhancement of AnNH uptake by the NO donor SNP (Table II) was due to increased apparent V_{max} values (up to 170% of the control value), without changes in the apparent K_m . Conversely, the alkylating agent PMSF reduced the apparent V_{max} to 50% of the control, without changing the apparent K_m (Table III). It is tempting to suggest that the active site of the transporter may contain a cysteine residue, which could be the target of both NO donors and alkylating agents. The effect of co-incubation with PMSF strengthens this hypothesis.

Altogether, the results reported here form the first characterization of human brain FAAH. In addition, the observations highlight the possible role of linoleoyl analogues of AnNH (and hydro(pero)xides generated thereof and from AnNH itself by lipoxygenase activity) as inhibitors of human brain FAAH. The AnNH transporter also has been characterized for the first time in human cells, showing that it was not affected by the AnNH derivatives/analogues that inhibited FAAH, but was sensitive to NO donors.

These findings give rise to a general picture of the inactivation process of AnNH in human neuronal and immune cells (Scheme 1). AnNH is brought into the cell by a transporter protein and is rapidly cleaved by intracellular FAAH. Lipoxygenase-generated products of AnNH can competitively inhibit FAAH, which affords an elevated intracellular AnNH concentration. The resulting dissipation of the AnNH gradient renders the transporter inactive and leads to an enlarged extracellular anandamide concentration. Enhanced CB receptor stimulation results in prolonged pharmacological activity. On the other hand, the enhanced CB receptor-induced NO formation potentiates the transporter protein, which clears AnNH from the extracellular space. The NO-stimulated accumulation of AnNH might be further enhanced by the fact that short pulses of NO are able to inhibit lipoxygenase activity (30), thus preventing inhibition of FAAH by lipoxygenase-generated hydroperoxides of AnNH and congeners. Interestingly, any signaling pathway leading to NO release, either coupled or not coupled to cannabinoid receptors, might affect AnNH metabolism by activating AnNH (re)uptake. In this perspective, CB1 and/or CB2 receptors might reside on the same cell bearing the sequestration machinery or on different cells. The autocoid local inflammation antagonism (41) and the glutamate excitotoxicity on neurons (42), where AnNH exerts a(n)tagonistic effects on cannabinoid receptors and nitric oxide is released (10, 43), might be two relevant processes in which the proposed

sequestration scheme is operational. It is noteworthy that lipooxygenase activity is found in processes such as lymphocyte activation and neuronal cell death, where lipooxygenase activation (44, 45) might prolong the effects of AnNH (13).

Acknowledgments—We are grateful to Prof. R. Giuffrè and Dr. G. De Caro for kindly donating human brain specimens, to Prof. G. Bagetta and Dr. A. M. Paoletti ("Mondino-Tor Vergata" Center for Experimental Neurobiology, University of Rome Tor Vergata) for the binding assay carried out on CHP100 cells, to Guus van Zadelhof for the kind gift of 11- and 15-H(P)AnNH, and to Dr. E. Faggioni for the U937 cells.

REFERENCES

- Devane, W. A., Hannus, L., Breuer, A., Pertwee, R. G., Stevenson, L. A., Griffin, G., Gibson, D., Mandelbaum, A., Etinger, A., and Mechoulam, R. (1992) *Science* **258**, 1946–1949
- di Tomaso, E., Beltramo, M., and Piomelli, D. (1996) *Nature* **382**, 677–678
- Di Marzo, V., Fontana, A., Cadas, H., Schinelli, S., Cimino, G., Schwartz, J.-C., and Piomelli, D. (1994) *Nature* **372**, 686–691
- Sasaki, T., and Chang, C. J. (1997) *Life Sci.* **61**, 1803–1810
- Ueda, N., Kurahashi, Y., Yamamoto, S., and Tokunaga, T. (1995) *J. Biol. Chem.* **270**, 23823–23827
- Paria, B. C., Deutsch, D. D., and Dey, S. K. (1996) *Mol. Reprod. Dev.* **45**, 183–192
- Pertwee, R. G. (1997) *Pharmacol. Ther.* **74**, 129–180
- Derkinderen, P., Toutant, M., Burgaya, F., Le Bert, M., Siciliano, J. C., de Francis, V., Gelman, M., and Girault, J.-A. (1996) *Science* **273**, 1719–1722
- Wartmann, M., Campbell, D., Subramanian, A., Burstein, S. H., and Davis, R. J. (1995) *FEBS Lett.* **359**, 133–136
- Stefano, G. B., Liu, Y., and Goligorsky, M. S. (1996) *J. Biol. Chem.* **271**, 19238–19242
- Hillard, C. J., Edgemond, W. S., Jarrahan, A., and Campbell, W. B. (1997) *J. Neurochem.* **69**, 631–638
- Beltramo, M., Stella, N., Calignano, A., Lin, S. Y., Makriyannis, A., and Piomelli, D. (1997) *Science* **277**, 1094–1097
- Bisogno, T., Maurelli, S., Melck, D., De Petrocellis, L., and Di Marzo, V. (1997) *J. Biol. Chem.* **272**, 3315–3323
- Natarajan, V., Schmid, P. C., Reddy, V., and Schmid, H. H. O. (1987) *J. Neurochem.* **42**, 1613–1619
- Hillard, C. J., Wilkinson, D. M., Edgemond, W. S., and Campbell, W. B. (1995) *Biochim. Biophys. Acta* **1257**, 249–256
- Ueda, N., Yamamoto, K., Yamamoto, S., Tokunaga, T., Shirakawa, E., Shinkai, H., Ogawa, M., Sato, T., Kudo, F., Inoue, K., Takizawa, H., Nagano, T., Hirobe, M., Matsuki, N., and Saito, H. (1995) *Biochim. Biophys. Acta* **1254**, 127–134
- Maurelli, S., Bisogno, T., De Petrocellis, L., Di Lucia, A., Marino, G., and Di Marzo, V. (1995) *FEBS Lett.* **377**, 82–86
- Cravatt, B. F., Giang, D. K., Mayfield, S. P., Boger, D. L., Lerner, R. A., and Gilula, N. B. (1996) *Nature* **384**, 83–87
- Giang, D. K., and Cravatt, B. F. (1997) *Proc. Natl. Acad. Sci. U. S. A.* **94**, 2238–2242
- Corasaniti, M. T., Melino, G., Navarra, M., Garaci, E., Finazzi Agrò, A., and Nisticò, G. (1995) *Neurodegeneration* **4**, 315–321
- Galiègue, S., Mary, S., Marchand, J., Dussosoy, D., Carriere, D., Carayon, P., Bouaboula, M., Shire, D., Le Fur, G., and Casellas, P. (1995) *Eur. J. Biochem.* **232**, 54–61
- Van der Stelt, M., Paoletti, A. M., Maccarrone, M., Nieuwenhuizen, W. F., Bagetta, G., Veldink, G. A., Finazzi Agrò, A., and Vliegthart, J. F. G. (1997) *FEBS Lett.* **415**, 313–316
- Van der Stelt, M., Nieuwenhuizen, W. F., Veldink, G. A., and Vliegthart, J. F. G. (1997) *FEBS Lett.* **411**, 287–290
- Mechoulam, R., Frider, E., Hanus, L., Sheskin, T., Bisogno, T., Di Marzo, V., Bayewitch, M., and Vogel, Z. (1997) *Nature* **389**, 25–26
- Segel, I. H. (1976) *Biochemical Calculations*, pp. 277–281, John Wiley & Sons, Inc., New York
- Maccarrone, M., Veldink, G. A., and Vliegthart, J. F. G. (1991) *J. Biol. Chem.* **266**, 21014–21017
- Robertson, E. F., Dannelly, H. K., Malloy, P. J., and Reeves, H. C. (1987) *Anal. Biochem.* **167**, 290–294
- Maccarrone, M., Nieuwenhuizen, W. F., Dullens, H. F. J., Catani, M. V., Melino, G., Veldink, G. A., Vliegthart, J. F. G., and Finazzi Agrò, A. (1996) *Eur. J. Biochem.* **241**, 297–302
- Zamzami, N., Marchetti, P., Castedo, M., Decaudin, D., Macho, A., Hirsch, T., Susin, S. A., Petit, P. X., Mignotte, B., and Kroemer, G. (1995) *J. Exp. Med.* **182**, 367–377
- Maccarrone, M., Corasaniti, M. T., Guerrieri, P., Nisticò, G., and Finazzi Agrò, A. (1996) *Biochem. Biophys. Res. Commun.* **219**, 128–133
- Matthews, J. R., Botting, C. H., Panico, M., Morris, H. R., and Hay, R. T. (1996) *Nucleic Acids Res.* **24**, 2236–2242
- Kurahashi, Y., Ueda, N., Suzuki, H., Suzuki, M., and Yamamoto, S. (1997) *Biochem. Biophys. Res. Commun.* **237**, 512–515
- Perry, A., Stafford, S. L., Scheithauer, B. W., Suman, V. J., and Lohse, C. M. (1997) *Am. J. Surg. Pathol.* **21**, 1455–1465
- Hampson, A. J., Hill, W. A. G., Zan-Phillips, M., Makriyannis, A., Leung, E., Eyles, R. M., and Bornheim, L. M. (1995) *Biochim. Biophys. Acta* **1259**, 173–179
- Valk, P., Verbakel, S., Vankan, Y., Hol, S., Mancham, S., Ploemacher, R., Mayen, A., Lowenberg, B., and Delwel, R. (1997) *Blood* **90**, 1448–1457
- Derocq, J. M., Bouaboula, M., Marchand, J., Rinaldi-Carmona, M., Segui, M., and Casellas, P. (1998) *FEBS Lett.* **425**, 419–425
- Giros, B., El Mestikawy, S., Bertrand, L., and Caron, M. G. (1991) *FEBS Lett.* **295**, 149–154
- Robinson, M. B., Hunter-Ensor, M., and Sinor, J. (1991) *Brain Res.* **544**, 196–202
- Schaffer, J. E., and Lodish, H. F. (1994) *Cell* **79**, 427–436
- Kanai, N., Lu, R., Satriano, J. A., Bao, Y., Wolkoff, A. W., and Schuster, V. L. (1995) *Science* **268**, 866–869
- Facci, L., Dal Toso, R., Romanello, S., Buriani, A., Skaper, S. D., and Leon, A. (1995) *Proc. Natl. Acad. Sci. U. S. A.* **92**, 3376–3380
- Skaper, S. D., Buriani, A., Dal Toso, R., Petrelli, L., Romanello, S., Facci, L., and Leon, A. (1996) *Proc. Natl. Acad. Sci. U. S. A.* **93**, 3984–3989
- Montague, P. R., Gancayco, C. D., Winn, M. J., Marchase, R. B., and Friedlander, M. J. (1994) *Science* **263**, 973–977
- Los, M., Schenk, H., Hexel, K., Baeuerle, P. A., Droge, W., and Schulze-Osthoff, K. (1995) *EMBO J.* **14**, 3731–3740
- Maccarrone, M., Catani, M. V., Finazzi Agrò, A., and Melino, G. (1997) *Cell Death Differ.* **4**, 396–402
- Genetics Computer Group, Inc. (1994) *Program Manual for the GCG Sequence Analysis Software Package*, Version 8, Genetics Computer Group, Inc., Madison, WI